AFM and neurodegenerative diseases (part I): Correlating Atomic Force Microscopy (AFM) and Fluorescence Microscopy to detect changes in cell morphology caused by protein aggregates of mutant Huntingtin

By: Alexandre Berquand, Ph.D.,
Life Science Application Scientist
Veeco Instruments GmbH

Andreas Holloschi, Dipl. Ing. Biotechnology,
Sandra Ritz, Dipl. Ing. Biotechnology,
Mathias Hafner, Prof. Dr., Petra Kioschis,
Prof. Dr., Mannheim University of
Applied Science, Institute of Molecular
and Cell Biology

In the present study, the BioScope™ II Atomic Force Microscope has been integrated with epifluorescence for the identification and characterization of huntingtin aggregates in CHO-K1 (Chinese Hamster Ovary) cells.

INTRODUCTION

Atomic Force Microscopy (AFM)[1] operates by scanning a sharp tip, supported on a sensitive force-sensing cantilever, over the sample and thereby producing a three-dimensional image of the surface. As the tip scans across the samples, changes in the interactions with the surface alter the vertical deflection of the tip. These changes in deflection are monitored via an optical detection method. A feedback control system responds to those changes by adjusting the tip-sample distance in order to maintain a constant deflection. It is this vertical movement of the tip that is used to produce a topographical image of the surface. Both contact mode and TappingMode™ have demonstrated their high value in life sciences applications, especially during the 5 past years.

The high resolution imaging capability of AFM has recently facilitated the construction of atomic models of supramolecular assemblies from topographical images of photosynthetic proteins[2] and channel proteins.[3] Furthermore, great progress has been made in the use of AFM for live cell imaging.[4,5] One of the most remarkable advancements of AFM in the field of life science, however, is the application of force spectroscopy studies on live cells under near-physiological conditions.[6-9]

Force spectroscopy allows investigation of single molecule recognition processes, cell dynamics and mechanical properties at a high spatial resolution and high force sensitivity. Recently, AFM force studies have been successfully applied to the study of neurodegenerative diseases such as Alzheimer's and Huntington's diseases.[10-12]

COMBINING AFM WITH OPTICAL MICROSCOPY

Conducting an AFM force spectroscopy experiment is inherently a statistical process. As such, these studies often require many control experiments to be performed in order to confidently attribute observed interactions to specific binding of the ligand and receptors of interest. By combining AFM with optical microscopy, we can overcome some of these issues and offer new features such as identification and localization of molecules/ receptors of interest and targeted force measurements.

In the present paper, we will focus our attention on Huntington's disease, a progressive autosomal dominant disorder which is caused by expansion of the glutamine tract of huntingtin (htt) and leads to psychiatric, motor and cognitive impairments. The mechanism underlying the cause of this disease remains unclear, although multiple pathologic mechanisms have been proposed.[13]

As in all polyglutamine disorders, Huntington's Disease is characterized pathologically by the presence of polyglutamine protein containing intracellular aggregates. Here we use

the unique capabilities of the Bioscope™ II combined with an inverted optical microscope to perform live cell studies of the cellular effects caused by mutant huntingtin assembling in intracellular protein aggregates. We will also highlight the imaging capabilities of our tool, especially the combination of AFM and fluorescence imaging of cells. In the second paper of this two-part series on atomic force microscopy of neurodegenerative diseases, we will emphasize the force spectroscopy capabilities of the BioScope II.

SAMPLE PREPARATION

CHO-K1 cells were transfected with YFP-tagged huntingtin exon 1 fragment (HttexQ68-EYFP,AS 1-90; 68 polyglutamines). Transfection was performed using 2 x10^5 cells, 1 µg plasmid DNA, and 3 µl Fugene HD (Roche) per well. Subsequently, cells were seeded on sterile cover slips (18x18 mm) in 6-well plates. After 24-48h incubation cells were washed twice with PBS and fixed with 4% PFA for 10 min.

Brightfield (BF), Differential Interference Contrast (DIC) and epifluorescence images were recorded using a Zeiss Axio Observer equipped with AxioCam MRc camera and AxioVision software. All AFM images were recorded on a Veeco Bioscope II using MLCT and DNP-20 cantilevers. The system combining AFM and optical measurements was used as a fully integrated tool. All experiments were performed in contact and TappingMode™ in PBS buffer. 3D-rending of the AFM height images was performed, using Veeco's VISION software package.

REGISTRATION AND CORRELATION OF AFM AND OPTICAL DATA

For proper registration and correlation of AFM and optical data it is critical to have the ability to align the AFM tip within the optical field of view, as well as position the tip relative to a region of interest on a sample.

The availability of both a manual and motorized XY-translation stage on the BioScope II provides an easy and efficient means of tip/optics and tip/sample alignment. Starting at low magnification — this affords a larger field of view of both the sample and AFM tip position — huntingtin aggregates are clearly detectable by various optical contrasting techniques; in BF, in epifluorescence based on the strong fluorescent signal mediated by the YFP-tagged htt, and in DIC based on the aggregates of htt which change cell topology.

We start with positioning the AFM tip in the center of the field of view using the manual X-Y translation stage (important for when switching to higher magnification – and hence smaller field of view). Then we use the motorized stage to position a region of interest relative to tip. This way both the tip and the region of interest are typically at the center of the field of view.

In Figure 1, we show an example of this situation: Images 1A and 1B show the BF and the fluorescence images of the selected area, respectively, but the cantilever is not located in this display window (the shape of the tip is visible on the right bottom corner of image 1A). Using successively manual and motorized stages, it is extremely easy to move the tip just above the area of interest.

Positioning both the tip and region of interest in the center of the optical field of view will also help to minimize some optical aberrations/warping effects that could affect the accuracy of image registration. These aberrations (chromatic and spherical) are more prevalent nearer the outer edges of the field of view for a particular objective and minimal in/around the optical axis.

The design of the BioScope II's motorized stage is extremely stable, and aids in obtaining highly accurate images. The three motor screws of the Bioscope II do not rotate, unlike most AFM's; instead, the motor screws move straight in and out of the head. This provides a "no wobble" approach of the AFM tip, helping to maintain accurate targeting of a region of interest on the sample during the engage process. The NanoScope® V Controller's software-automated engage procedure provides a quick but safe engagement of the tip on the sample surface. This is crucial when imaging soft samples — for preservation of both the sample and the AFM tip.

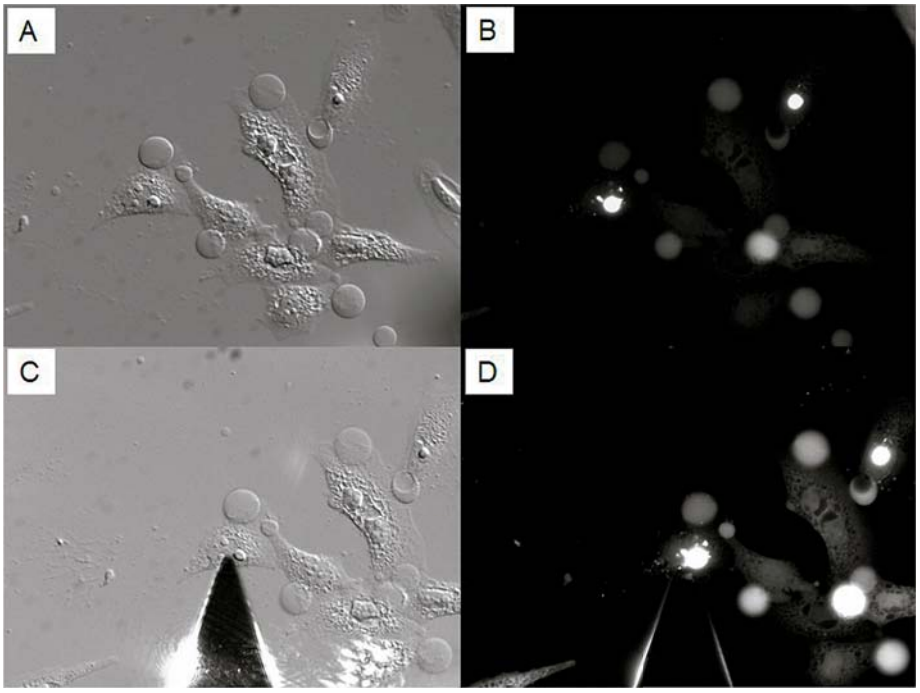

Figure 1: Reaching the area of interest using the "Navigate" function. In A (bright field image) and B (fluorescence image), some bright htt aggregates that are of interest are visible but the tip is both far away from the sample and out of the field of view (see shadow on the right bottom corner of image A). Using the X, Y motion screws and the joystick allows placement of the tip on top of the area of interest (C and D,bright field and fluorescence image, respectively.). Optical images obtained with a 20x objective.

Images 1C (BF) and 1D (fluorescence) were taken at the very final step of the approach procedure. Interestingly, the IR laser used for AFM detection has no perturbing effects on BF or epifluorescence images. The IR superluminescent diode does not interfere with red biological fluorophores. At 850 nm, it can also be easily filtered if a customer has an IR-sensitive camera and wants to remove the observed spilling of the laser light around the AFM tip from their optical images.

Figure 2 is a direct example of the type of studies that are enabled by combined AFM and fluorescence imaging. Figures 2A, 2B and 2C, which correspond to BF, DIC, and fluorescence respectively, show aggregates of mutant huntingtin. The arrows in the images indicate the specific aggregate selected for scanning with the AFM tip whereas the region outlined in red specifies the scanning area of the AFM tip. Image 2D shows a three dimensional AFM topography image of the cells within the outlined region in the corresponding optical images.

The huntingtin protein aggregate observed by optical microscopy (yellow arrow) is also easily observed in the AFM image (red arrow). While the presence of various aggregates on the surface of the cells are easily observed by AFM, topography imaging alone does not allow you to distinguish between different types of aggregates (besides the YFP-tagged aggregates other cellular substructures influencing cell topology were detected in the AFM scan [Images 2A, 2B and 2D green arrows]). By combining AFM with optical microscopy, the presence/absence of a fluorescent signal in correlated fluorescence images allows one to accurately identify if an aggregate is composed of the huntingtin proteins or not.

Note that some cells exhibit homogeneous fluorescent cellular staining that is due to the presence of soluble huntingtin protein throughout the cell cytoplasm. In contrast, mutant huntingtin proteins already accumulated in aggregates exhibit

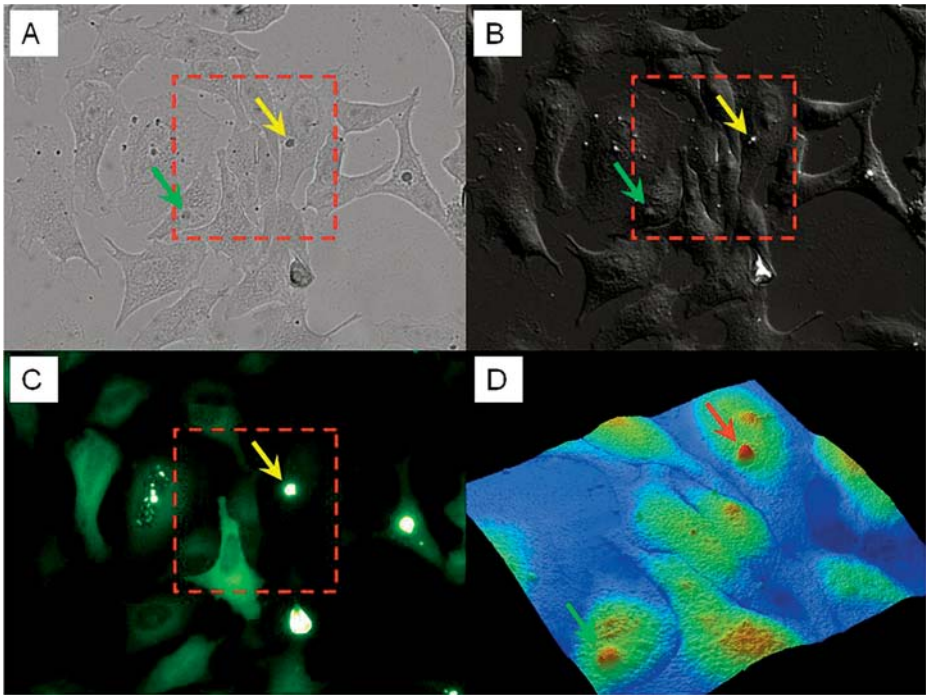

Figure 2: Using AFM to generate additional information to optical microscopy. Mutant YFP-tagged htt protein forms bright aggregates (images A, bright field and B, DIC, image C, epifluorescence, yellow arrows) that are also easily recognized in the AFM topographic channel (image D, red arrow in). In addition, changes in cell topology caused by other cellular substructures similar to that caused by aggregates could also be detected by the AFM scan (image D, green arrow). Optical images taken with a 20x objective. AFM scan: 90x90x3µm.

locally very strong fluorescence and are thus easy to identify.

Images were collected using various objectives with a magnification range from 20x to 100x, as well as a high numerical aperture 100x TIRF objective. However, due to the strong fluorescence intensity of the huntingtin aggregates, best results were obtained by epifluorescence with a 20x objective.

RESULTS: HUNTINGTIN AGGREGATES REMARKABLY HETEROGENEOUS

After a complete series of experiments, cross section analysis performed in the NanoScope software revealed the huntingtin aggregates remarkably heterogeneous in size and shape, from a few hundred nanometers up to several microns (~4 µm) in diameter. Friction images (data not shown) revealed a contrast between the aggregates and the bulk of the cell.

Phase images, collected in TappingMode (data not shown), also exhibited an interesting phase contrast in the region of the aggregates. Relative phase changes (or contrast) across a sample can often indicate differences in surface properties, such as viscoelasticity or electrostatic charge distribution. Thus, a phase contrast in areas corresponding to the aggregates would indicate that they are made up of material or components that are different than that of the surrounding cell surface.

We also investigated cells expressing wild type form of huntingtin (data not shown). In this case, huntingtin proteins remain soluble and thus, no changes of cell topology mediated by huntingtin aggregates were detected.

CONCLUSION

In the present study, the imaging capabilities of the BioScope II were integrated with fluorescence microscopy to locate and image protein aggregates of mutant huntingtin, a characteristic hallmark of Huntington's Disease. This application indicates the high selectivity and accuracy of the combined system in the 3D identification of molecules in biological systems and investigation of their physical properties through optical imaging and topographic, friction, viscoelastic, and adhesion

measurements. This technology opens a wide range of applications in the comprehensive functional analysis of nanomolecular complexes in living cells and their relevance in disease onset and progression as well as in testing the physiological effects of new compounds in drug discovery.

REFERENCES:

1. G. Binnig, C. F. Quate & C. Gerber 1986
   Atomic Force Microscope
   Phys. Rev. Lett. 56: 930-933.
2. S. Scheuring, T. Boudier & J. N. Sturgis 2007
   From high-resolution AFM topographs to atomic models of supramolecular assemblies.
   J. Struct. Biol. 159: 268-276.
3. S. Scheuring, N. Buzhynskyy, S. Jaroslawski, R. P. Goncalves, R. K. Hite & T. Waltz 2007
   Structural models of the supramolecular organization of AQP0 and connexons in junctional microdomains.
   J. Struct. Biol. 160: 385-394.
4. L. Kreplak, H. Wang, U. Aebi & x. P. Kong 2007
   Atomic force microscopy of Mammalian urothelial surface.
   J. Mol. Biol. 374: 365-373.
5. S. G. Kaminskij & T. E. Dahms 2007
   High spatial resolution surface imaging and analysis of fungal cells using SEM and AFM.
   Micron (under press)
6. M. Radmacher, M. Fritz, C. M. Kacher, J. P. Cleveland & P. K. Hansma 1996
   Measuring the viscoelastic properties of human platelets with the atomic force microscope.
   Biophys. J. 70: 556-567.
7. V. Dupres, C. Verbelen & Y. Dufrene 2007
   Probing molecular recognition sites on biosurfaces using AFM.
   Biomaterials 28: 2393-2402.
8. F. Gaboriaud & Y. Dufrene 2007
   Atomic force microscopy of microbial cells: application to nanomechanical properties, surface forces and molecular recognition forces.
   Colloids Surf. B Biointerfaces 54: 10-19.
9. T. G. Kuznetsova, M. N. Starodubtseva, N. I. Yegorenkov, S. A. Chizhik & R. I. Zhdanov 2007
   Atomic force microscopy probing of cell elasticity.
   Micron 38: 824-833.
10. P. R. Dahlgren, M. A. Karymov, J. Bankston, T. Holden, P. Thumfort, V. M. Ingram & Y. L. Lyubchenko 2005
    Atomic force microscopy analysis of the Huntington protein nanofibril formation.
    Nanomedicine 1: 52-57.
11. Y. Li, M. Cao & Y. Wang 2006
    Alzheimer amyloid beta(1-40) peptide: interactions with cationic gemini and single-chain surfactants.
    J. Phys. Chem. B 110: 18040-18045.
12. H. Jang, J. Zheng & R. Nussinov 2007
    Models of beta-amyloid ion channels in the membrane suggest that channel formation in the bilayer is a dynamic process.
    Biophys. J. 93: 1938-1949.
13. E. Cattaneo, C. Zuccato & M. Tartari. 2005
    Normal huntingtin function: an alternative approach to Huntington's disease.
    Nature Reviews Neuroscience 6: 919-930

WORLDWIDE CUSTOMER SUPPORT FROM THE INDUSTRY LEADER

Bruker Corporation is a leading provider of high-performance scientific instruments and solutions for molecular and materials research, as well as for industrial and applied analysis. For more information, visit www.bruker.com, email productinfo@bruker-nano.com, or call +1.805.967.1400/800.873.9750.